Virology 532 (2019) 48–54

Contents lists available at ScienceDirect

Virology

journal homepage: www.elsevier.com/locate/virology

Identification of a human respiratory syncytial virus phosphoprotein domain required for virus-like-particle formation

Chetan D. Meshram[b], Antonius G.P. Oomens[a,*]

[a] Center for Veterinary Health Sciences, Oklahoma State University, 250 McElroy Hall, Stillwater, OK, 74078, USA
[b] Department of Microbiology. University of Alabama at Birmingham, Birmingham, AL, USA

ARTICLE INFO

Keywords:
Respiratory syncytial virus
Virus-like-particle
Assembly
Phosphoprotein

ABSTRACT

Perceived inefficiency and inadequate knowledge of the human respiratory syncytial virus (hRSV) assembly process present a hurdle for large-scale production of authentic hRSV virus-like particles (VLPs) for vaccine purposes. We previously established that the matrix protein, phosphoprotein (P), and fusion protein carboxy-terminus were sufficient to generate VLPs that resemble filamentous wildtype hRSV. Here, the contribution of P was examined. By co-expressing matrix, fusion, and modified P proteins, a ser/thr-rich P region (residues 39–57) was found to be critical for VLP formation, whereas the oligomerization domain was not. Substitutions throughout region 39–57 inhibited VLP formation and relevant amino acids were identified. Phosphomimetic substitutions of serines and threonines inhibited VLP formation; Phosphoblatant substitutions did not. The data show that P not only co-regulates replication and transcription but also has an important role in assembly, mediated by a separate domain that likely interacts with M and/or F and is highly regulated by phosphorylation.

1. Introduction

More than one human respiratory syncytial virus (hRSV) vaccine or vaccine strategy may be necessary to address divergent requirements associated with age, health, and immune status. One of the strategies for hRSV vaccine development is based on virus-like particles (VLPs). VLPs can resemble a wildtype (wt) virus morphologically and structurally but lack the viral genome. They can efficiently deliver antigens, and induce both Th2 and Th1 based responses due to cross-presentation (Bachmann and Jennings, 2010; Grgacic and Anderson, 2006; Jennings and Bachmann, 2008). Two distinct heterologous VLPs (based on Newcastle disease virus [NDV] or Influenza virus) carrying RSV glycoproteins were shown to induce a response that was not only safe and protective, but also more durable than that induced by wt hRSV (Lee et al., 2015; McGinnes Cullen et al., 2015; Schmidt et al., 2012; Schmidt et al., 2014). Thus, VLPs have potential to induce relevant and durable immune responses without the risk of viral replication and associated virulence. In the past few years, the first successful VLP vaccines (human papilloma virus, hepatitis B virus) have been brought to market. All anti-hRSV VLP vaccines currently in preclinical development are based on foreign viral systems incorporating the hRSV glycoproteins. This is in part due to the availability of heterologous VLP systems, to the perceived inefficiency of hRSV VLP production, and to insufficient understanding of hRSV particle assembly. Homologous, authentic, hRSV VLPs, if they can be produced at sufficient levels, will accurately mimic the viral morphology and structure and can include internal hRSV proteins which tend to be relatively well conserved, thereby increasing the breadth of the response and its ability to protect across strains. Our long-term goal is to understand the mechanisms that govern hRSV particle formation, to ultimately learn to produce authentic hRSV VLPs and live-attenuated viruses to specifications and purities suitable for large-scale vaccination. Identification of the minimal players involved in particle assembly is an important step in this process.

In cell culture, the majority of infectious hRSV particles remain associated with the cell surface and have a filamentous character (Bachi and Howe, 1973; Gower et al., 2005; Kiss et al., 2014; Liljeroos et al., 2013; Norrby et al., 1970; Roberts et al., 1995; Ke et al., 2018; Oomens et al., 2003; Utley et al., 2008). However, manipulation or purification of particles can lead to morphological changes in the particle and conformational changes in the F protein. To avoid such changes, we study VLP assembly requirements by examining the surface of transfected cells co-expressing viral proteins. The information gained is relevant also because cell culture represents an important platform by which future VLP and live virus -based vaccines will be generated. Using the transfected cell system, we previously established by scanning electron microscopy (SEM) that of the 11 known hRSV proteins, co-expression of only three proteins (matrix protein M, fusion protein F,

* Corresponding author. Center for Veterinary Health Sciences, Oklahoma State University, 258 McElroy Hall, Stillwater, OK, 74078, USA.
E-mail addresses: meshram@uab.edu (C.D. Meshram), oomens@okstate.edu (A.G.P. Oomens).

https://doi.org/10.1016/j.virol.2019.04.001
Received 22 December 2018; Received in revised form 3 April 2019; Accepted 4 April 2019
Available online 09 April 2019
0042-6822/

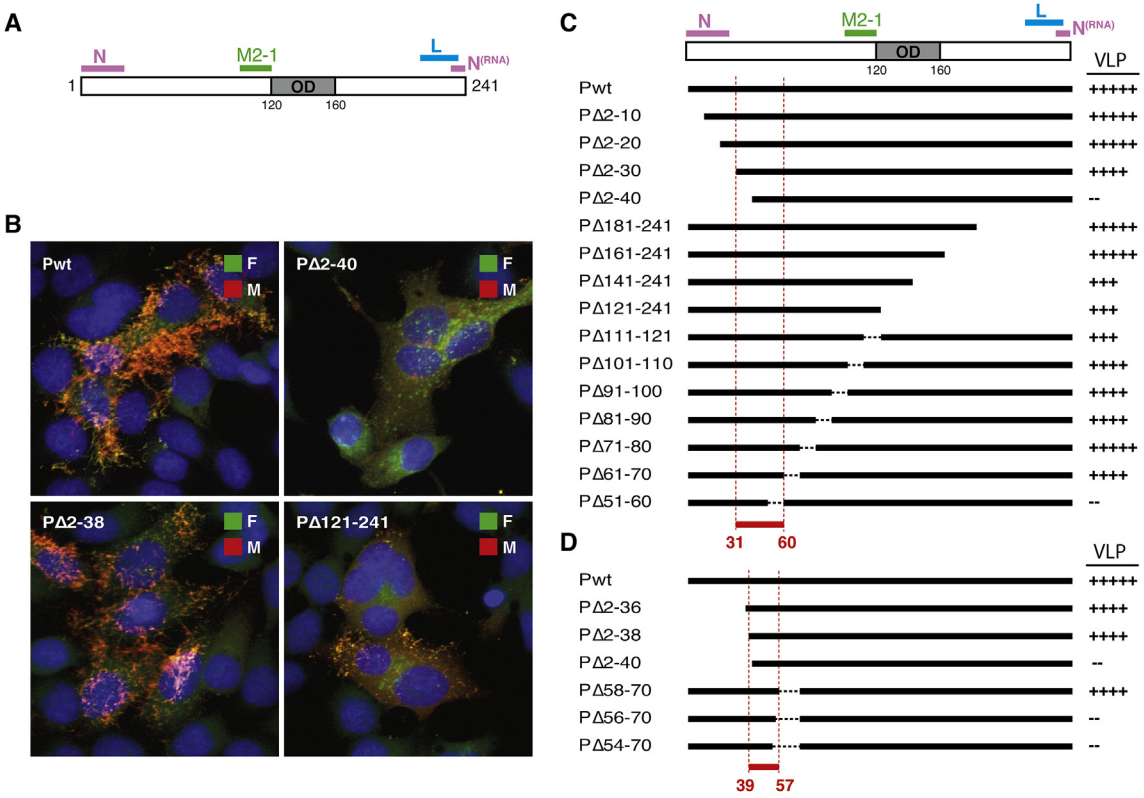

Fig. 1. Preliminary mapping of the P region required for VLP assembly: Amino acids 39–57 play a critical role (Fig. 1A). Diagram of hRSV P protein structure and function. Bars represent domains shown to be involved in interactions with N, N-encapsidated RNA, M2-1, and L. OD = oligomerization domain (Fig. 1B–D). Impact of P modifications on P-M-F induced VLP formation in transfected cells. HEp-2 cells were co-transfected with plasmids expressing F, M, and various P modifications, and fixed and permeabilized at 22 hpt as described previously (Meshram et al., 2016). Cells were blocked and incubated with anti-M (Mitra et al., 2012) and anti-F (Synagis) antibodies, followed by rabbit or human secondary antibodies conjugated with alexa-568 (M) or 488 (F) respectively. Cells were counterstained with DAPI and scored for relative amounts of filamentous VLP formation by assigning a score from 1 to 5 based on five independent fields examined at 100x magnification (Fig. 1C). A few representative samples were photographed at 600 x magnification (Fig. 1B). In Fig. 1D, additional P modifications were applied to more narrowly map the region involved in VLP assembly.

and phosphoprotein P) was sufficient for relatively abundant formation of morphologically accurate, filamentous viral particles (Meshram et al., 2016). Moreover, for F, only the carboxy-terminus (transmembrane domain [TMD] and cytoplasmic tail [CT]) were required. In absence of P, M and F formed a type of rudimentary particle that was longer and thinner than a wt particle and could not be harvested from cell culture either due to low abundance or poor structural integrity. The requirement for P to obtain a wt virus-resembling particle, pointed to an unexpected role for P in VLP assembly and morphology.

Although the atomic structure of hRSV P has not been resolved, P was shown to be a homo-tetramer with an elongated shape (Castagne et al., 2004; Llorente et al., 2006, 2008; Pereira et al., 2017). hRSV P is smaller than the P proteins of paramyxoviruses, but the general organization appears similar and shows a central coiled-coil oligomerization domain (OD) (Castagne et al., 2004; Llorente et al., 2008; Asenjo and Villanueva, 2000) flanked by intrinsically disordered N− and C-termini (Pereira et al., 2017; Bruhn et al., 2014; Esperante et al., 2012; Galloux et al., 2015; Karlin et al., 2003; Pickar et al., 2015; Simabuco et al., 2011). The shape and disordered nature of the flanking domains are believed to contribute to the ability of the relatively small P protein to interact with several viral proteins and carry out multiple functions (Pereira et al., 2017; Karlin et al., 2003; Simabuco et al., 2011). Most functions pertain to viral replication and transcription, for which the roles of P as a cofactor have been extensively documented. To carry out its replication-related roles, P interacts with the nucleoprotein N and N-RNA complexes (Castagne et al., 2004; Galloux et al., 2015; Garcia-Barreno et al., 1996; Tawar et al., 2009; Tran et al., 2007), anti-terminator protein M2-1 (Esperante et al., 2012; Asenjo et al., 2006; Mason et al., 2003; Tran et al., 2009), and polymerase protein (L) (Khattar et al., 2001; Sourimant et al., 2015). To regulate its multiple functions and interactions, P phosphorylation plays an important role and appears to be complex, with several potential sites identified throughout the protein (Castagne et al., 2004; Asenjo et al., 2005, 2008a; Lu et al., 2002). However, phosphorylation is not required for oligomerization of P, and the impact of overall phosphorylation status on replication and transcription is not clear but appears to be minimal (Castagne et al., 2004; Asenjo and Villanueva, 2000; Galloux et al., 2015; Lu et al., 2002; Villanueva et al., 2000).

Some of the first evidence for a role for P not directly related to viral replication/transcription was provided by Lu et al. (2002) and Asenjo et al. (2005). In particular, phosphomimetic substitution of P residue serine 54 (S54) was found to increase the number of sites where P and M co-localize during an early stage of the hRSV entry process, suggestive of a block in uncoating. S54 also appeared to be involved in an interaction with the M protein that facilitated formation of a low level of 'membranous vesicles' (in the context of vaccinia virus), whereas interaction with N or L was not affected by S54 phosphorylation status (Asenjo et al., 2005, 2008a). These previous findings, and our observation that P plays a critical role in VLP production and particle morphology (Meshram et al., 2016), led us to further investigate P and map the P domain involved in VLP assembly.

To identify P domains involved in P-M-F driven VLP assembly, we constructed a large number of P variants with amino-terminal, carboxy-terminal, or internal, truncations. These P variants were examined in previously established qualitative and quantitative VLP formation assays, in which P, M, and F are transiently co-expressed. Collectively, the

study identifies a serine/threonine-rich 19 amino acid region within the P domain (residues 39–57) that is critical for VLP assembly.

2. Results

An immunofluorescence based assay identifies a region with major impact on VLP production. For several unrelated viruses, matrix-like proteins are an important structural component and the major driving force behind particle formation. The interactions and functions that drive hRSV particle formation are poorly understood. We previously reported that in addition to hRSV M protein, the P and F proteins are required to generate VLPs that closely resemble wt filamentous virions by SEM (Meshram et al., 2016). We also determined that for F, only the carboxy-terminal domain was required. Since P is believed to have a modular character which allows it to interact with multiple viral proteins (Fig. 1A) (Pereira et al., 2017; Karlin et al., 2003), we anticipated that a separate domain may be responsible for the contribution of P to VLP assembly. In line with our goals to identify the players and interactions that govern hRSV particle assembly, the P protein was dissected.

A large number of stepwise P truncations (amino-terminal, carboxy-terminal, as well as internal) were generated and transiently coexpressed with M and F proteins in HEp-2 cells. We utilized a previously described immunofluorescence microscopy (IFM) based assay (Meshram et al., 2016) to provide an initial assessment of the impact of P truncations on VLP formation (Fig. 1). The IFM assay is not quantitative but readily distinguishes large differences in the level of VLP production between samples (Meshram et al., 2016), and served as a pre-screen. Briefly, HEp-2 cells were transfected with plasmids expressing M, F and P or P protein variants, and fixed at 24 hpt. Fixed cells were permeabilized to enable fluorescent labeling of the M protein, in addition to F. Cell surfaces were examined for VLP formation and assigned a score from 1 to 5 based on five independent fields examined at 100x magnification (Fig. 1B and C). Fig. 1B shows examples of the results using wt P, as well as samples with a high, low, or intermediate level of VLPs. In absence of an Ab to detect all forms, we did not verify P protein levels. However, protein levels of relevant mutants were verified in Fig. 2 based on a flag tag, showing that, in agreement with previous work on P mutations, even extensive P modifications have little impact on protein level. Analysis of P truncations showed that the majority induced wt or near-wt levels of VLPs. The area with the strongest impact on VLP formation was the area from residue 31 to 60. Additional mutants in the identified region were generated and subjected to the same assay to more narrowly define the relevant amino acids (Fig. 1D). The results showed that only amino acids 39–57 were required for VLP formation. P39-57 is a serine/threonine-rich region in the N-terminal domain, that also contains S54, a residue previously implicated in viral uncoating (Asenjo et al., 2008b). The P carboxy-terminal half was largely dispensable for VLP formation. However, absence of the previously reported OD (~residues 121–160) (Castagne et al., 2004; Llorente et al., 2008), had a minor negative impact on the level of VLPs.

Quantitating the impact of P modifications on VLP formation: only P residues 39–57 are required for VLP formation. To quantitate the impact of P modifications, the above as well as additional P mutations, were tested in a previously established western blot-based VLP assay (Fig. 2). In this VLP assay, cells were co-transfected with M, F, and P, or P mutants, and processed at 24 hpt. Cells were washed, collected by scraping, and VLPs were isolated by gentle pipetting the cell suspension up and down, and removal of cells and cell debris by low-speed centrifugation. VLPs were then pelleted through a 20% sucrose cushion at high g-force. Protein content of the harvested VLPs was examined using quantitative western blots after reducing SDS-PAGE. The mutants of P in addition to those used in Fig. 1, were variants that contained only the two domains that had an impact on VLP production (residues 39–57 and the OD, residues 121–160), to ask whether this minimal construct could still support VLP production. Residues 58–60 were also included to provide some spacing between the two domains. Note that due to absence of an Ab that can cleanly detect P and all of the truncated forms on western blot, we used flag tags both at the amino-terminus (Pflag2) and the carboxy-terminus (Pflag240) (see Fig. 2A). Preliminary data showed that flag-tagged wt P supported VLP formation as well as untagged wt P (not shown).

First, to verify expression levels, HEp-2 cells were transfected with plasmids expressing modified P proteins (without M and F co-expression), and cell extracts were examined on western blot (Fig. 2B). Both Pflag2 and Pflag240 expressed to high level. Consistent with previous publications, P truncations and deletions did not interfere with P expression. Next, the constructs shown in Fig. 2A were subjected to the VLP assay (Fig. 2C). As before, VLPs were quantitated based on the level of M, because M is the central organizer of particle assembly (Meshram et al., 2016; McPhee et al., 2011). Consistent with Fig. 1 we found that PΔ2–40 and PΔ56–70 were strongly reduced in their capacity to support VLP formation, whereas PΔ2–38 and PΔ58–70 were not, pointing to P region 39–57 as a critical domain. All other mutants generated near wt levels of VLPs, with the exception of mutant PΔ2–38/61-120/160–241 (residues 39–60 coupled to the OD) which had an intermediate phenotype. Addition of residues 111–120 to mutant PΔ2–38/61-120/160–241 restored the level of VLPs to wt. The latter may indicate that residues 111–120 help P oligomerize, that additional spacing is required in between these two functional domains, or that an unknown P function associated with residues 111–120 is required for P to function optimally in this assay.

When we quantified P levels when co-expressed with M and F (Fig. 2C; bottom panel) it appeared, in contrast to Fig. 2B, that expression levels varied between mutants. However, mutants PΔ61–70 and PΔ58–70 showed poor expression levels yet efficiently supported VLP production. Since P is essential for VLP production, this suggests that normal levels are present of these P mutants, in agreement with Fig. 2B. In an unrelated Ab test of MAb RSV-P-4 (Antibodies Online) we found that it readily recognized wt P on western when expressed alone, but very poorly recognized P when co-expressed with M and F (not shown). Together with previous work from other groups, these observations suggest that P tolerates extensive modification without compromising expression level; However, co-expression with M and F leads to differential recognition on western blots, presumably via post-translational modifications that occur only, or are different, when other viral proteins are present. This would be consistent with a protein that is extensively regulated by phosphorylation/dephosphorylation to expose or hide functional domains to carry out multiple interactions.

Analysis of P region 39–57. To determine the impact of individual amino acids of the 39–57 region on VLP assembly, we carried out an alanine scanning analysis using Pflag2. Because some residues in this region have previously been shown to be phosphorylated (Asenjo et al., 2005) and P in general is a highly phosphorylated protein, all six serine and threonine residues were also substituted with aspartic acid or glutamic acid, to mimic the phosphorylated state (Fig. 3A). P mutants were co-expressed with M and F, and harvested VLPs were analyzed as above. The results of non-serine and threonine substitutions are shown in Fig. 3B, the results of all serine and threonine substitutions in Fig. 3C. Prior to VLP analysis, all P mutants were expressed in cells to verify expression level, using GAPDH as a control. Two mutations (S42D and E53A) expressed poorly, and hence no conclusions were made regarding these residues. The VLP data (co-expression of M, F, and P) are shown in the original non-normalized format because expression levels of P mutations (except S42D, P53A) were highly similar to wt P. In addition, Fig. 2 suggested that the level of detected P mutants can be drastically altered in the presence of M and F, making it difficult to ascertain the P levels and normalize based on P in co-transfected samples. The VLP data show that many residues in the 39–57 region partially impacted VLP formation. Substitution of residues I46, I48, and E49 to alanine reduced VLP production by 60–65% (Fig. 3B).

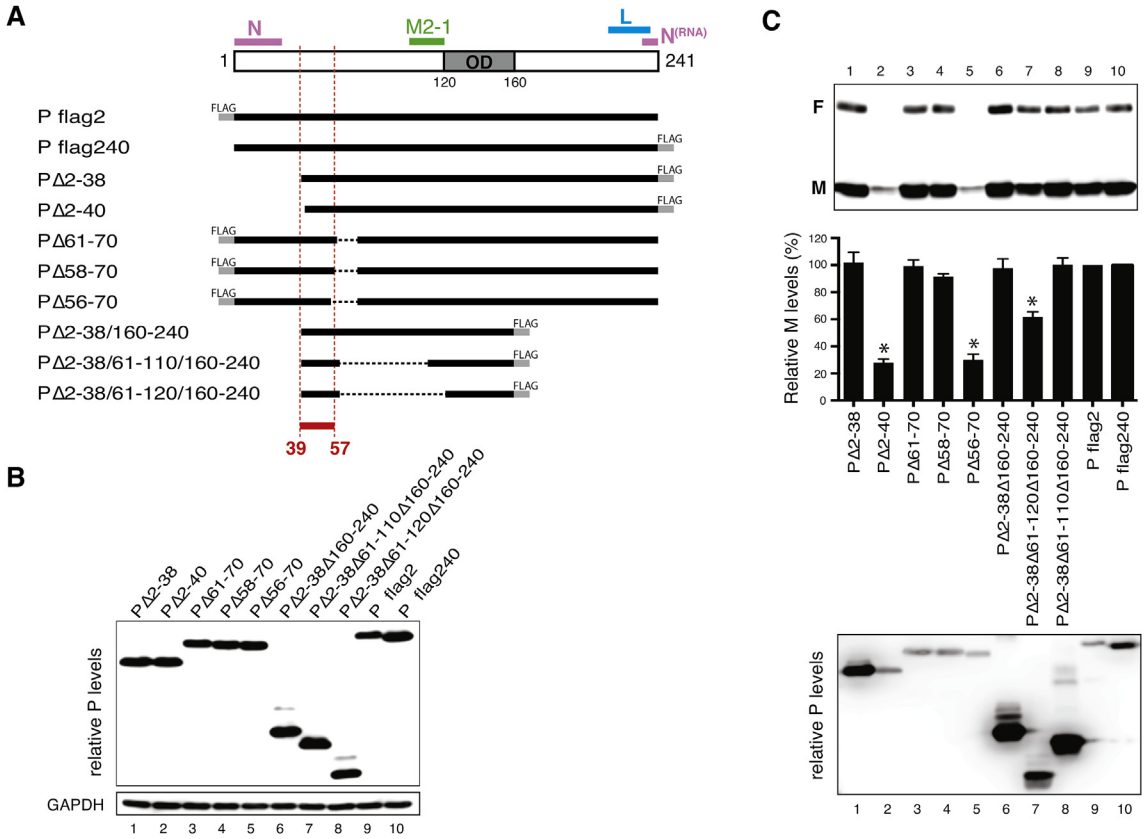

Fig. 2. Impact of P modifications on P-M-F induced VLP formation: A minimal construct consisting of P amino acids 39–60 coupled to the OD induces high levels of VLP formation (Fig. 2A). Modified P proteins with flag tags at the amino- or carboxy-terminus were used to quantitate the impact on VLP formation (Fig. 2B). Relative expression levels of modified P proteins in the absence of other viral proteins in HEp-2 cells at 24 hpt (detected by anti-Flag antibodies) (Fig. 2C). Impact of P modifications on P-M-F induced VLP formation in transfected cells. HEp-2 cells were co-transfected with plasmids expressing F, M, and various P modifications, and VLP formation was assessed at 24 hpt as described previously (Meshram et al., 2016). VLPs were harvested after clearing cell debris and pelleting at high g-force through a sucrose cushion. VLPs were subjected to reducing SDS-PAGE and western blots were generated. The amount of M protein was quantitated by a C-DiGit scanner and software (LI-COR) as an indicator of VLPs produced. Please note that lanes 7 and 8 are reversed compared to Fig. 2B. Values represent the mean and standard deviation from three independent experiments. *P $<$ 0.05 (unpaired two-tailed *t*-test).

Substitution of residue N44 to alanine reduced VLP production by 85–90%. The most impactful non-serine/threonine residues were I40 and I56, which almost completely abrogated VLP production when mutated to alanine. Interestingly, serine and threonine subsitutions to alanine had no to minor impact, whereas substitutions of these same residues with phosphomimetic amino acids lowered VLP production by at least 60% (Fig. 3C). Notably, phosphomimetic mutations S39D, S54D, and S57D severely impacted VLP formation ($\leq$5% of wt P). Together, the data identify I40, I56, S39, S54, and S57 as the most critical residues. For the latter three, the impact is likely mediated by their phosphorylation state. The finding that alanine substution of serines and threonines supports VLP production much better than phosphomimetic substitutions suggests that any assembly-related functions of this domain are probably carried out in an unphosphorylated state.

3. Discussion

In previous work, we found that P played an unexpected role in assembly and morphology. Whereas its role in RNA replication has been extensively examined, very little is known about assembly functions of P. P was shown to be an intrinsically disordered protein with separate regions interacting with N, N associated with RNA, M2-1, and L (Castagne et al., 2004; Esperante et al., 2012; Galloux et al., 2015; Garcia-Barreno et al., 1996; Tawar et al., 2009; Tran et al., 2007, 2009; Asenjo et al., 2006; Mason et al., 2003; Khattar et al., 2001; Sourimant et al., 2015). Based on these findings, we hypothesized that P may have a separate domain involved in particle assembly, and performed a mutational analysis to map this domain. A region was identified (amino acids 39–57) that is critical for VLP assembly and likely to have a complex phosphorylation-dependent regulation to ensure that the many P functions are carried out in proper spacio-temporal fashion.

P residues 39–57 play an important role in particle assembly. As a first step, using immunofluorescence microscopy we looked for P truncations that blocked formation of filamentous VLPs, and identified one region with major impact. These results were then confirmed and extended by harvesting VLPs and quantitation on western blots. N-terminal truncation beyond residue 38 almost completely abrogated VLP formation (Fig. 2). Similarly, truncation from the carboxy-terminal side beyond residue 57 severely lowered VLP formation, thereby establishing area 39–57 as a domain required for efficient VLP assembly, henceforth referred to as assembly domain (AD). Although we have not directly tested whether the AD expressed alone can carry out its assembly functions, coupling amino acids 39–60 to the previously established oligomerization domain (120–160) or an extended version thereof (110–160) supported VLP formation at 60 and 100% respectively, relative to wt P. Removal of the entire or partial OD, while leaving the N-terminal half of P intact, had only a minor impact on VLP formation (Fig. 1). Together these data suggest that the AD is the only P domain critical for particle assembly, and its assembly functions are independent of the L, M2-1, and N interacting domains. Oligomerization may improve efficiency, but the combined data suggest it is not required. The same was true for the oligomerization status of P in its role in RNA replication (Asenjo et al., 2008a).

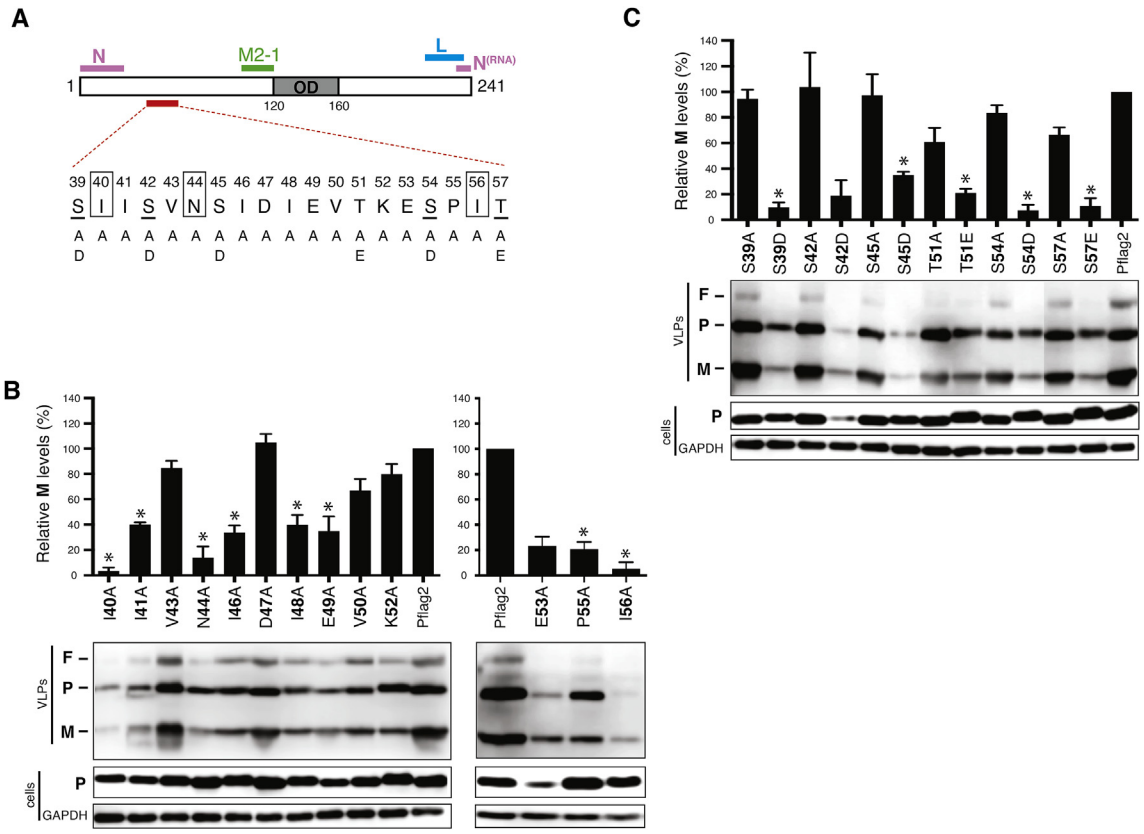

Fig. 3. Impact of individual amino acids 39–57 on P-M-F induced VLP formation (Fig. 3A). Diagram of amino acid content of the identified assembly region. Rectangles indicate non-ser/thr residues with largest impact on VLP assembly; Underlined residues may play an important role in assembly function mediated by phosphorylation status (Fig. 3B). Impact of non-serine/threonine residues (Fig. 3C). Impact of serine/threonine residues. For Fig. 3C, both phosphablatant (alanine) and phosphomimetic substitutions (aspartic or glutamic acid) were examined. VLP formation was quantitated as in Fig. 2. *P $<$ 0.05 (compared to Pflag2; unpaired two-tailed *t*-test).

The contribution of individual amino acids and the role of phosphorylation. Residues with strong impact on VLP formation were found throughout the 39–57 region, suggesting that the entire region is involved in assembly-related functions by P. Among the non-ser/thr residues, amino acids I40, N44, and I56 were especially influential, each reducing VLP formation by more than 90%. This implies that these residues are key players in the interaction of P with M or the F carboxy-terminus. Other residues (I41, I46, I48, E49, and P55) partially inhibited VLP formation and may also contribute. The identified AD also contains six serine and threonine residues. Several groups have made previous efforts to map P phosphorylation sites. This was done under wide-ranging conditions and with varying results. However, residues 116, 117, and 232 in the OD and N binding domains respectively, were found to be phosphorylated in independent studies (Castagne et al., 2004; Galloux et al., 2015; Asenjo et al., 2005, 2008a; Lu et al., 2002), and studies also agreed that phosphorylation was not required for oligomerization of P. One study identified a residue in the 39–57 region with high-turnover phosphorylation: S54. Mutation of this serine to aspartic acid, which mimics the phosphorylated state, appeared to play a role in viral uncoating upon RSV entry (Asenjo et al., 2008b), and to interfere with formation of a low level of 'membranous vesicles' when P and M were co-expressed in the context of vaccinia-T7 virus (Asenjo et al., 2005). In addition, it was reported that (in the hRSV Long strain) mutation of S46 to alanine, led to phosphorylation of residues 30, 39, and 45, indicative of complex and potentially redundant phosphorylation. In our VLP assembly studies we found that phosphomimetic substitution of all serines and threonines (except S42D which had reduced expression levels) in the AD significantly and independently lowered VLP assembly, whereas phosphoblatant substitution (alanine) did not (Fig. 3). Although the data presented here do not prove that these amino acid residues are phosphorylated in the RSV life cycle, previous studies have shown phosphorylation of several residues within this region. Our data do indicate that all potential phosphorylation sites need to be in an unphosphorylated state in order for the AD to mediate particle assembly, and suggests that phosphorylation of any of the serines and threonines will render P incapable of supporting assembly. Phosphorylation status may represent a factor in the switch between transcription/replication and assembly modes of P. Along these lines, phosphorylation of AD residues upon entry may represent a step in the disassembly of the particle and switching on the transcription related functions of P. In support of this scenario, a kinase (glycogen synthase kinase 3β) capable of phosphorylating S54 was shown to be packaged in the viral particle (Asenjo et al., 2008b).

Multiple studies show that modifications of P have little impact on P expression level, which enables mutagenesis analyses. This is consistent with the intrinsic disorder of the P protein. However, we found that, when expressed in the context of M and F, different P mutants are no longer evenly detected. This is true even for flag-tagged P whether flag is placed amino-terminally or carboy-terminally (Fig. 2). In agreement with this is our finding that a commerially available Ab (RSV-P-4, Antibodies Online) recognizes wt P efficiently when expressed alone, but poorly when co-expressed with M and P. Together these findings suggest that P undergoes extensive conformational rearrangements mediated by M or F. This would be consistent with a protein that interacts with multiple viral proteins in distinct functions, and with the complex phosphorylation of P. It makes it difficult however, to ascertain P protein levels in the context of transient co-expression with M and F or in the viral context, regardless of the Ab used. The direct impact of modifications on P expression levels is therefore best verified by expressing P in the absence of other viral proteins.

In conclusion: A 19 amino acid ser/thr-rich assembly domain was identified that mediates VLP formation in an unphosphorylated state. Besides a potentially direct role for (unphosphorylated) serines and threonines, residues I40, N44, I56 were the amino acids most critical for VLP assembly and likely to be involved in interactions with M and F.

Together with previously described N, M2-1, and L interacting domains, which are also influenced by phosphorylation, P appears to have a complex phosphorylation-dependent functional regulation, including the newly identified AD. Oligomerization of the AD may contribute to its function but is not required, and AD function is independent of the N, M2-1, and L interacting domains. A study with bovine P protein showed that deletion of amino acids 41–60 enhanced minigenome replication (Khattar et al., 2001), and thus the AD may not only promote assembly but also impede transcription or replication. Similarly, phosphorylation status of the AD may contribute to the switch between transcription/replication and assembly modes of P, and be involved in the trigger for disassembly after entry.

The identified AD in P partially overlaps with a P region previously predicted to be disordered (amino acids 47–77) (Whelan et al., 2016), and fits previous characterizations of P as a multifunctional intrinsically disordered protein. Such domains generally allow high specificity, low affinity interactions (Simabuco et al., 2011) which would be required for P in order to engage and disengage other viral proteins. Identification of a relatively small AD further confirms the importance of M as a central constituent and player in the formation of RSV particles. We can now conclude that in addition to M, only two small domains appear to be required for efficient VLP formation: the F carboxy-terminus and P residues 39–57. Since M and F form aberrant viral filaments in absence of P (Meshram et al., 2016), and P and M were reported to form a low level of 'membranous vesicles' in absence of F (Asenjo et al., 2005), it appears that the P AD and the F carboxy-terminus can each independently interact with M. Both co-factors however are required for M to form a particle shell that morphologically resembles a wt virion, and this process may also involve host factors. Knowing the minimal players will help map the unknown interactions that govern RSV particle assembly, which will prove beneficial for large-scale VLP and live virus production for vaccine purposes, and may identify targets for drug intervention.

4. Materials and methods

Cells and primary antibodies. HEp-2 cells were acquired from the American Type Culture Collection and grown in standard DMEM advanced medium (Gibco) containing 5% FBS. The following monoclonal antibodies were used for immunofluorescence and/or immunoblotting: Synagis (anti-F) was provided by MedImmune, Inc. Mab19 (anti-F) was provided by Ed Walsh (University of Rochester School of Medicine). Anti-flag antibody was acquired from Genscript. A rabbit polyclonal anti-M peptide serum was reported previously (Mitra et al., 2012).

Plasmid constructs for transfection. The M, F, and P expressing plasmids used for transfection in HEp-2 cells were previously reported (Meshram et al., 2016; Mitra et al., 2012; Baviskar et al., 2013). The N− and C-terminal deletions and internal deletions of P, as well as point mutations, were generated by site-directed mutagenesis. To generate Pflag2 and Pflag240, the flag epitope (DYKDDDDK) were inserted at amino acid positions 2 and 240, respectively, of the P ORF using site-directed mutagenesis.

Fluorescence microscopy. To detect VLPs by immunofluorescence microscopy, a previously established method was used (Meshram et al., 2016). Briefly, HEp-2 cells were grown on glass coverslips and transfected using lipofectin, for 4 h at 37C. At 22 h post removal of transfection solution (hpt), cells were fixed with freshly dissolved 4% paraformaldehyde for 20 min and permeabilized for 5 min with 0.1% SDS. Following blocking with 1% BSA, cells were incubated with anti-flag (to detect P), anti-M, or anti-F (Synagis) antibodies. The cells were labeled with secondary antibodies conjugated with alexa-488 or 568, washed, counterstained with DAPI and photographed at 600 x magnification on a Nikon TE2000 inverted fluorescence microscope with a DS-Qi1 and DS-U2 camera controller. Images were processed using Adobe Photoshop CS5.1.

Quantitative VLP assay. VLPs were harvested and the viral protein levels were quantitated as reported previously (Meshram et al., 2016) with minor modifications. At 16 hpt, the medium of transfected cells was replaced with reduced serum medium (OPTI-MEM, Invitrogen), and cells incubated for an additional 8 h. At 24 hpt, cells were collected using a rubber cell scraper. The collected cell suspension was agitated gently by pipetting up and down with a pipetman, and cell debris was removed by centrifugation for 5 min at $800 \times g$. VLP-containing supernatants were overlaid on a 20% sucrose cushion and VLPs were pelleted by centrifugation for 45 min at high g-force. Supernatants were discarded and pellets (containing VLPs) were resuspended and boiled in 1x Laemli buffer. Samples were resolved on 12% reducing SDS-PAGE gels and transferred to immobilon blots using a semi-dry western blot apparatus (Bio-Rad). Blots were incubated with anti-M, anti-F (MAb19) or anti-flag antibodies (to detect P), followed by a horseradish peroxidase-conjugated secondary antibodies. Blots were developed using ECL substrate (Pierce) and scanned on a C-DiGit Blot scanner (LI-COR Biosciences). M bands on western blots were quantitated using C-DiGit Image Studio Software. As an indicator of amounts of VLP produced, the relative amounts of M in the VLP fractions were calculated by dividing the amount of M in each sample to the amount of M in control samples Pflag2 or Pflag240, which were set at 100%. The final reported values (relative M protein level) represent the mean and standard deviation of at least three independent experiments. Statistical significance was determined by unpaired two-tailed student's t-test.

Funding

This work was supported by the National Institute of General Medical Sciences, National Institutes of Health (P20GM103648).

ACKOWLEDGMENTS

We thank the members of the Oomens Laboratory for helpful discussions during the preparation of the manuscript.

References

Asenjo, A., Villanueva, N., 2000. Regulated but not constitutive human respiratory syncytial virus (HRSV) P protein phosphorylation is essential for oligomerization. FEBS Lett. 467, 279–284.

Asenjo, A., Rodriguez, L., Villanueva, N., 2005. Determination of phosphorylated residues from human respiratory syncytial virus P protein that are dynamically dephosphorylated by cellular phosphatases: a possible role for serine 54. J. Gen. Virol. 86, 1109–1120.

Asenjo, A., Calvo, E., Villanueva, N., 2006. Phosphorylation of human respiratory syncytial virus P protein at threonine 108 controls its interaction with the M2-1 protein in the viral RNA polymerase complex. J. Gen. Virol. 87, 3637–3642.

Asenjo, A., Mendieta, J., Gomez-Puertas, P., Villanueva, N., 2008a. Residues in human respiratory syncytial virus P protein that are essential for its activity on RNA viral synthesis. Virus Res. 132, 160–173.

Asenjo, A., Gonzalez-Armas, J.C., Villanueva, N., 2008b. Phosphorylation of human respiratory syncytial virus P protein at serine 54 regulates viral uncoating. Virology 380, 26–33.

Bachi, T., Howe, C., 1973. Morphogenesis and ultrastructure of respiratory syncytial virus. J. Virol. 12, 1173–1180.

Bachmann, M.F., Jennings, G.T., 2010. Vaccine delivery: a matter of size, geometry, kinetics and molecular patterns. Nat. Rev. Immunol. 10, 787–796.

Baviskar, P.S., Hotard, A.L., Moore, M.L., Oomens, A.G., 2013. The respiratory syncytial virus fusion protein targets to the perimeter of inclusion bodies and facilitates filament formation by a cytoplasmic tail-dependent mechanism. J. Virol. 87, 10730–10741.

Bruhn, J.F., Barnett, K.C., Bibby, J., Thomas, J.M., Keegan, R.M., Rigden, D.J., Bornholdt, Z.A., Saphire, E.O., 2014. Crystal structure of the Nipah virus phosphoprotein tetramerization domain. J. Virol. 88, 758–762.

Castagne, N., Barbier, A., Bernard, J., Rezaei, H., Huet, J.C., Henry, C., Da Costa, B., Eleouet, J.F., 2004. Biochemical characterization of the respiratory syncytial virus P-P and P-N complexes and localization of the P protein oligomerization domain. J. Gen. Virol. 85, 1643–1653.

Esperante, S.A., Paris, G., de Prat-Gay, G., 2012. Modular unfolding and dissociation of the human respiratory syncytial virus phosphoprotein p and its interaction with the m(2-1) antiterminator: a singular tetramer-tetramer interface arrangement. Biochemistry 51, 8100–8110.

Galloux, M., Gabiane, G., Sourimant, J., Richard, C.A., England, P., Moudjou, M., Aumont-Nicaise, M., Fix, J., Rameix-Welti, M.A., Eleouet, J.F., 2015. Identification and characterization of the binding site of the respiratory syncytial virus phosphoprotein to RNA-free nucleoprotein. J. Virol. 89, 3484–3496.

Garcia-Barreno, B., Delgado, T., Melero, J.A., 1996. Identification of protein regions involved in the interaction of human respiratory syncytial virus phosphoprotein and nucleoprotein: significance for nucleocapsid assembly and formation of cytoplasmic inclusions. J. Virol. 70, 801–808.

Gower, T.L., Pastey, M.K., Peeples, M.E., Collins, P.L., McCurdy, L.H., Hart, T.K., Guth, A., Johnson, T.R., Graham, B.S., 2005. RhoA signaling is required for respiratory syncytial virus-induced syncytium formation and filamentous virion morphology. J. Virol. 79, 5326–5336.

Grgacic, E.V., Anderson, D.A., 2006. Virus-like particles: passport to immune recognition. Methods 40, 60–65.

Jennings, G.T., Bachmann, M.F., 2008. The coming of age of virus-like particle vaccines. Biol. Chem. 389, 521–536.

Karlin, D., Ferron, F., Canard, B., Longhi, S., 2003. Structural disorder and modular organization in Paramyxovirinae N and P. J. Gen. Virol. 84, 3239–3252.

Ke, Z., Dillard, R.S., Chirkova, T., Leon, F., Stobart, C.C., Hampton, C.M., Strauss, J.D., Rajan, D., Rostad, C.A., T, J.V., Yi, H., Shah, R., Jin, M., Hartert, T.V., Peebles Jr., R.S., Graham, B.S., Moore, M.L., Anderson, L.A., Wright, E.R., 2018. The morphology and assembly of respiratory syncytial virus revealed by cryo-electron tomography. Viruses 10.

Khattar, S.K., Yunus, A.S., Collins, P.L., Samal, S.K., 2001. Deletion and substitution analysis defines regions and residues within the phosphoprotein of bovine respiratory syncytial virus that affect transcription, RNA replication, and interaction with the nucleoprotein. Virology 285, 253–269.

Kiss, G., Holl, J.M., Williams, G.M., Alonas, E., Vanover, D., Lifland, A.W., Gudheti, M., Guerrero-Ferreira, R.C., Nair, V., Yi, H., Graham, B.S., Santangelo, P.J., Wright, E.R., 2014. Structural analysis of respiratory syncytial virus reveals the position of M2-1 between the matrix protein and the ribonucleoprotein complex. J. Virol. 88, 7602–7617.

Lee, Y.N., Hwang, H.S., Kim, M.C., Lee, Y.T., Lee, J.S., Moore, M.L., Kang, S.M., 2015. Recombinant influenza virus expressing a fusion protein neutralizing epitope of respiratory syncytial virus (RSV) confers protection without vaccine-enhanced RSV disease. Antivir. Res. 115, 1–8.

Liljeroos, L., Krzyzaniak, M.A., Helenius, A., Butcher, S.J., 2013. Architecture of respiratory syncytial virus revealed by electron cryotomography. Proc. Natl. Acad. Sci. U. S. A. 110, 11133–11138.

Llorente, M.T., Garcia-Barreno, B., Calero, M., Camafeita, E., Lopez, J.A., Longhi, S., Ferron, F., Varela, P.F., Melero, J.A., 2006. Structural analysis of the human respiratory syncytial virus phosphoprotein: characterization of an alpha-helical domain involved in oligomerization. J. Gen. Virol. 87, 159–169.

Llorente, M.T., Taylor, I.A., Lopez-Vinas, E., Gomez-Puertas, P., Calder, L.J., Garcia-Barreno, B., Melero, J.A., 2008. Structural properties of the human respiratory syncytial virus P protein: evidence for an elongated homotetrameric molecule that is the smallest orthologue within the family of paramyxovirus polymerase cofactors. Proteins 72, 946–958.

Lu, B., Ma, C., Brazas, R., Jin, H., 2002. The major phosphorylation sites of the respiratory syncytial virus phosphoprotein are dispensable for virus replication in vitro. J. Virol. 76, 10776–10784.

Mason, S.W., Aberg, E., Lawetz, C., DeLong, R., Whitehead, P., Liuzzi, M., 2003. Interaction between human respiratory syncytial virus (RSV) M2-1 and P proteins is required for reconstitution of M2-1-dependent RSV minigenome activity. J. Virol. 77, 10670–10676.

McGinnes Cullen, L., Schmidt, M.R., Kenward, S.A., Woodland, R.T., Morrison, T.G., 2015. Murine immune responses to virus-like particle associated pre- and post-fusion forms of the respiratory syncytial virus F protein. J. Virol. https://doi.org/10.1128/jvi.00384-15.

McPhee, H.K., Carlisle, J.L., Beeby, A., Money, V.A., Watson, S.M., Yeo, R.P., Sanderson, J.M., 2011. Influence of lipids on the interfacial disposition of respiratory syncytical virus matrix protein. Langmuir 27, 304–311.

Meshram, C.D., Baviskar, P.S., Ognibene, C.M., Oomens, A.G., 2016. The respiratory syncytial virus phosphoprotein, matrix protein, and fusion protein carboxy-terminal domain drive efficient filamentous virus-like particle formation. J. Virol. 90, 10612–10628.

Mitra, R., Baviskar, P., Duncan-Decocq, R.R., Patel, D., Oomens, A.G., 2012. The human respiratory syncytial virus matrix protein is required for maturation of viral filaments. J. Virol. 86, 4432–4443.

Norrby, E., Marusyk, H., Orvell, C., 1970. Morphogenesis of respiratory syncytial virus in a green monkey kidney cell line (Vero). J. Virol. 6, 237–242.

Oomens, A.G., Megaw, A.G., Wertz, G.W., 2003. Infectivity of a human respiratory syncytial virus lacking the SH, G, and F proteins is efficiently mediated by the vesicular stomatitis virus G protein. J. Virol. 77, 3785–3798.

Pereira, N., Cardone, C., Lassoued, S., Galloux, M., Fix, J., Assrir, N., Lescop, E., Bontems, F., Eleouet, J.F., Sizun, C., 2017. New insights into structural disorder in respiratory syncytial virus phosphoprotein and implications for binding of protein partners. J. Biol. Chem. 292, 2120–2131.

Pickar, A., Elson, A., Yang, Y., Xu, P., He, B., 2015. Oligomerization of mumps virus phosphoprotein. J. Virol. 89, 11002–11010.

Roberts, S.R., Compans, R.W., Wertz, G.W., 1995. Respiratory syncytial virus matures at the apical surfaces of polarized epithelial cells. J. Virol. 69, 2667–2673.

Schmidt, M.R., McGinnes, L.W., Kenward, S.A., Willems, K.N., Woodland, R.T., Morrison, T.G., 2012. Long-term and memory immune responses in mice against Newcastle disease virus-like particles containing respiratory syncytial virus glycoprotein ectodomains. J. Virol. 86, 11654–11662.

Schmidt, M.R., McGinnes-Cullen, L.W., Kenward, S.A., Willems, K.N., Woodland, R.T., Morrison, T.G., 2014. Modification of the respiratory syncytial virus f protein in virus-like particles impacts generation of B cell memory. J. Virol. 88, 10165–10176.

Simabuco, F.M., Asara, J.M., Guerrero, M.C., Libermann, T.A., Zerbini, L.F., Ventura, A.M., 2011. Structural analysis of human respiratory syncytial virus P protein: identification of intrinsically disordered domains. Braz. J. Microbiol. 42, 340–345.

Sourimant, J., Rameix-Welti, M.A., Gaillard, A.L., Chevret, D., Galloux, M., Gault, E., Eleouet, J.F., 2015. Fine mapping and characterization of the L polymerase-binding domain of the respiratory syncytial virus phosphoprotein. J. Virol.

Tawar, R.G., Duquerroy, S., Vonrhein, C., Varela, P.F., Damier-Piolle, L., Castagne, N., MacLellan, K., Bedouelle, H., Bricogne, G., Bhella, D., Eleouet, J.F., Rey, F.A., 2009. Crystal structure of a nucleocapsid-like nucleoprotein-RNA complex of respiratory syncytial virus. Science 326, 1279–1283.

Tran, T., Castagne, N., Bhella, D., Varela, P.F., Bernard, J., Chilmonczyk, S., Berkenkamp, S., Benhamo, V., Grznarova, K., Grosclaude, J., Nespoulos, C., Rey, F.A., Eleouet, J.F., 2007. The nine C-terminal amino acids of the respiratory syncytial virus protein P are necessary and sufficient for binding to ribonucleoprotein complexes in which six ribonucleotides are contacted per N protein protomer. J. Gen. Virol. 88, 196–206.

Tran, T., Castagne, N., Dubosclard, V., Noinville, S., Koch, E., Moudjou, M., Henry, C., Bernard, J., Yeo, R.P., Eleouet, J.F., 2009. The respiratory syncytial virus M2-1 protein forms tetramers and interacts with RNA and P in a competitive manner. J. Virol. 83, 6363–6374.

Utley, T.J., Ducharme, N.A., Varthakavi, V., Shepherd, B.E., Santangelo, P.J., Lindquist, M.E., Goldenring, J.R., Crowe Jr., J.E., 2008. Respiratory syncytial virus uses a Vps4-independent budding mechanism controlled by Rab11-FIP2. Proc. Natl. Acad. Sci. U. S. A. 105, 10209–10214.

Villanueva, N., Hardy, R.W., Asenjo, A., Yu, Q., Wertz, G.W., 2000. The bulk of the phosphorylation of human respiratory syncytial virus phosphoprotein is not essential but modulates viral RNA transcription and replication. J. Gen. Virol. 81, 129–133.

Whelan, J.N., Krishna, D.R., Uversky, V.N., Teng, M.N., 2016. Functional correlations of respiratory syncytial virus proteins to intrinsic disorder. Mol. Biosyst. 12, 1507–1526.